The Anti-angiogenic Activity of NSITC, a Specific Cathepsin L Inhibitor

ABDELHADI REBBAA[1], FEI CHU[2], THANGIRALA SUDHA[1], CHRISTINE GALLATI[1], USAWADEE DIER[1], EVGENY DYSKIN[1], MURAT YALCIN[1], CHRISTINE BIANCHINI[1], OLFAT SHAKER[3] and SHAKER A. MOUSA[1,4]

[1]*The Pharmaceutical Research Institute at Albany, Albany College of Pharmacy and Health Sciences, Rensselaer, NY;*
[2]*Children's Memorial Research Center, Department of Pediatrics, Northwestern University, Chicago, IL, U.S.A.;*
[3]*Cairo University, Cairo, Egypt;*
[4]*Vascular Vision Pharmaceuticals Co., Rensselaer, NY, U.S.A.*

Abstract. *Increased neovasculature and resistance to chemotherapy are hallmarks of aggressive cancer; therefore, the development of approaches to simultaneously inhibit these two processes is highly desirable. Previous findings from our laboratory have demonstrated that cathepsin L plays a key role in the development of drug resistance in cancer, and that its inhibition reversed this phenomenon. The goal of the present study was to determine whether targeting cathepsin L would inhibit angiogenesis. For this, the effects of a specific cathepsin L inhibitor, Napsul-Ile-Trp-CHO (NSITC), were tested in vitro on endothelial cell proliferation and interaction with the extracellular matrix, and also in vivo, by measuring its effect on angiogenesis in the chick chorioallantoic membrane (CAM) and mouse matrigel models. The results indicated that NSITC readily inhibits the proliferation of endothelial cells by inducing cell cycle arrest at the G_0/G_1 phase, and suppresses cell adhesion to different substrates. Investigation of the underlying mechanism(s) indicated that NSITC was able to reduce expression of the adhesion molecule $\alpha V\beta 3$ integrin, inhibit cathepsin L-mediated degradation of the extracellular matrix, and disrupt secretion of the pro-angiogenic factors fibroblast growth factor (FGF) and vascular endothelial growth factor (VEGF). NSITC demonstrated potent efficacy in inhibiting growth factor- and tumor mediated-angiogenesis in the CAM and mouse matrigel models of angiogenesis. The anti-angiogenic effects of NSITC resulted in inhibition of tumor growth in the CAM and in nude mouse xenograft models. Together, these findings provide evidence that cathepsin L plays an important role in angiogenesis and suggest that NSITC represents a potential drug for the treatment of aggressive cancer.*

Correspondence to: Shaker A. Mousa, Ph.D., MBA, FACC, FACB, The Pharmaceutical Research Institute at Albany, Albany College of Pharmacy and Health Sciences, 1 Discovery Drive, Room 238, Rensselaer, NY 12144, U.S.A. Tel: +1 5186947397, Fax: +1 5186947567, e-mail: Shaker.mousa@acphs.edu

Key Words: Cathepsin L, NSITC, angiogenesis, ECM, protease.

Angiogenesis is the generation of new blood vessels from preexisting microvasculature (1, 2). Because tumor growth and metastases depend on new blood vessel formation for their nutrient supply, angiogenesis has become an attractive target for cancer therapy (3, 4). Previous investigations indicated that metalloprotease-mediated degradation of cancer cell-associated extracellular matrix (ECM) plays a central role in facilitating microvessel sprouting within the tumor mass (5, 6). Accordingly, these enzymes were considered targets of choice for the development of therapeutics to inhibit angiogenesis (7). However, despite the fact that metalloproteinase inhibitors showed great promise *in vitro* and in preclinical studies, clinical trials using these agents were unsuccessful, due to poor efficacy and toxicity (8-10). As a result, research focus was re-directed toward investigating other ECM-degrading enzymes such as cathepsins (11-14). In recent years, cathepsin L has been of particular interest due to the finding that it plays an important role in cell survival, and thus in carcinogenesis (13, 15-17). The implication of cathepsin L in malignant transformation was elegantly demonstrated in a mouse model of multistage carcinogenesis, where deficiency of this enzyme was found to suppress tumor growth (18). In addition, previous findings from our laboratory have demonstrated that enhanced cathepsin L activity is not simply associated with cancer resistance to chemotherapy, but actually plays an active role in it (19, 20). Genetic approaches using antisense oligonucleotides against cathepsin L or engineered cancer cells that expressed single chain variable fragment (scFv) neutralizing antibodies (17)

were instrumental in validating the concept of targeting cathepsin L to treat aggressive tumors. The use of chemical inhibitors of cathepsin L to suppress the development of cancer resistance to chemotherapy (19, 20) provided further confirmation of this concept, and suggested that such agents might hold great promise for cancer treatment. The underlying mechanism(s) by which cathepsin L inhibition suppresses tumor growth is not yet fully understood, however, recent findings indicate that cellular susceptibility to senescence and/or 'visibility' to drugs may be enhanced (19, 20).

The discovery that cathepsin L participates in remodeling of the ECM (21) suggests that this enzyme might play a key role in angiogenesis. In the present study, we investigated the ability of NSITC, a specific cathepsin L inhibitor (19, 22), to inhibit angiogenesis *in vitro* and *in vivo*. Putative molecular mechanisms by which this inhibitor exerts its anti-angiogenic function were also studied.

Materials and Methods

Reagents. The cathepsin L inhibitor NSITC and recombinant enzyme were purchased from Biomol (Plymouth Meeting, PA, USA). Antibodies to αVβ3 integrin and β actin were obtained from Santa Cruz Biotechnology (Santa Cruz, CA, USA). FGF2 and VEGF were obtained from Invitrogen Life Technologies, Inc. (Carlsbad, CA, USA). Antibodies to FGF2, VEGF, granulocyte colony-stimulating factor (G-CSF), and monocyte chemotactic protein (MCP-1) used in the BioPlex assay were obtained from Bio-RAD (Hercules, CA, USA). Matrigel was purchased from BD Bioscience (San Jose, CA). Other chemicals and drugs were purchased from Sigma-Aldrich (St. Louis, MO, USA).

Cell culture. Human vascular endothelial cells (HUVECs) (Clonetics, San Diego, CA, USA) were maintained in endothelial growth medium (EGM) (Invitrogen) that was supplemented with bovine brain extract (12 μg/ml), recombinant human epidermal growth factor (10 ng/ml), 10% (v/v) heat-inactivated fetal bovine serum (FBS), hydrocortisone (1 μg/ml), 100 U/ml penicillin, 100 μg/ml streptomycin, and 2 mM L-glutamine. All culture additives were purchased from Invitrogen. Cultures were maintained in a 37˚C humidified chamber with 5% CO_2. Media was changed every 3 days and the cell lines were passaged at 80% confluence.

3-(4, 5-dimethylthiazolyl-2)-2, 5-diphenyltetrazolium bromide (MTT) assay. Cells were subjected to treatment with the cathepsin L inhibitor NSITC at concentrations ranging from 0 to 40 μM. After 48 hours of exposure to the drug, cell viability was determined by MTT viability assay, as described previously (23). Briefly, cells were seeded at a density of 10^4 cells/well in 96-well plates and then incubated with NSITC for 96 hours (h). Ten microliters of MTT solution (5 mg/ml) were added to each well and plates were incubated for 4 h at 37˚C. The cells were solubilized by the addition of 100 μl of 10% sodium dodecyl sulfate (SDS)/0.01 M HCl and incubated for 15 h at 37˚C. The optical density of each well was determined using an ELISA plate reader at an activation wavelength of 570 nm and reference wavelength of 650 nm. The percentage of viable cells was determined by comparison to untreated control cells.

Western blot. Cells were seeded in Dulbecco's modified Eagle's medium (DMEM) containing 10% FBS. After 24 h, NSITC was added at concentrations ranging from 0 to 40 μM and the cells were allowed to incubate for an additional 48 h. The cells were lysed in a solution of 50 mM HEPES pH 7.4, 150 mM NaCl, 100 mM NaF, 1 mM $MgCl_2$, 1.5 mM EGTA, 10% glycerol, 1% Triton ×100, 1 μg/ml leupeptin and 1 mM phenylmethylsulfonylfluoride. Equal quantities of protein were separated by 12% SDS polyacrylamide gel electrophoresis (PAGE), and then transferred to an Immobilon-P membrane. Proteins of interest were identified by sequential reaction of the membrane with anti-αVβ3 primary antibody, followed by horseradish peroxidase-conjugated anti-rabbit secondary antibody. Immunoreactive proteins were visualized by chemiluminescence.

Adhesion assay. The adhesion assay was performed as described previously (24) with some modifications. HUVECs were suspended in serum-free medium containing 0.1% dimethyl sulfoxide (DMSO) or different concentrations of NSITC. The cell suspension (2.5×10^5 cells in 0.5 ml of medium/well) was added to a 24-well plate pre-coated or not with matrigel or gelatin (0.5%), and cells were allowed to attach by incubation at 37˚C for 30 minutes (min). Unattached cells were removed by repeated washing with phosphate-buffered saline (PBS). Attached cells were stained with 0.5% crystal violet for 10 min. After washing with water, the stained cells were extracted with 0.25 ml of 10% acetic acid, and the absorbance of the dye extract was measured at 590 nm.

Cytokine secretion. The effect of NSITC on cytokine secretion was carried out using the BioPlex suspension assay system (Bio-Rad), according to the manufacturer's instructions. Briefly, beads coated with specific antibodies (anti-FGF2, -VEGF, -G-CSF or -MCP-1) were immobilized on a 96-well plate and then allowed to react with samples containing unknown amounts of cytokine. After a series of washes to remove unbound protein, a biotinylated detection antibody specific for a different epitope on the cytokine was added to the plate. Streptavidin-PE was added to the wells, and the reaction was quantified based on bead color and fluorescence intensity. Cytokine concentrations were calculated using BioPlex Manager software (Bio-Rad).

Cathepsin L-mediated degradation of matrigel. Cleavage of matrigel by purified cathepsin L was measured by incubating 10 μg of the substrate with 50 ng of the enzyme in 50 μl of reaction buffer (100 mM sodium acetate pH 5, 1 mM EDTA, and 4 mM dithiothreitol). Increasing doses of NSITC were added to the samples, and after incubation for 20 min at room temperature, proteins were denatured by the addition of 50 μl of Laemmeli buffer. Samples were boiled for 2 min, and then proteins were separated by SDS-PAGE. Proteins were visualized by Coomassie blue staining and photographed.

Angiogenesis and tumor growth in the CAM model. Ten-day-old chick embryos were purchased from SPAFAS (Preston, CT, USA) and maintained at 37˚C and 55% relative humidity. CAM assays were performed as previously described (25-27). A hypodermic needle was used to make a small hole in the blunt end of the egg shell, with a second hole then made on the broad side of the egg over an avascular portion of the embryonic membrane. Mild suction was applied to the first hole to displace the air sac so that the CAM dropped away from the shell. Using a Dremel drill (Racine, WI, USA), a 1.0-cm^2 window was cut in the shell over the false air sac,

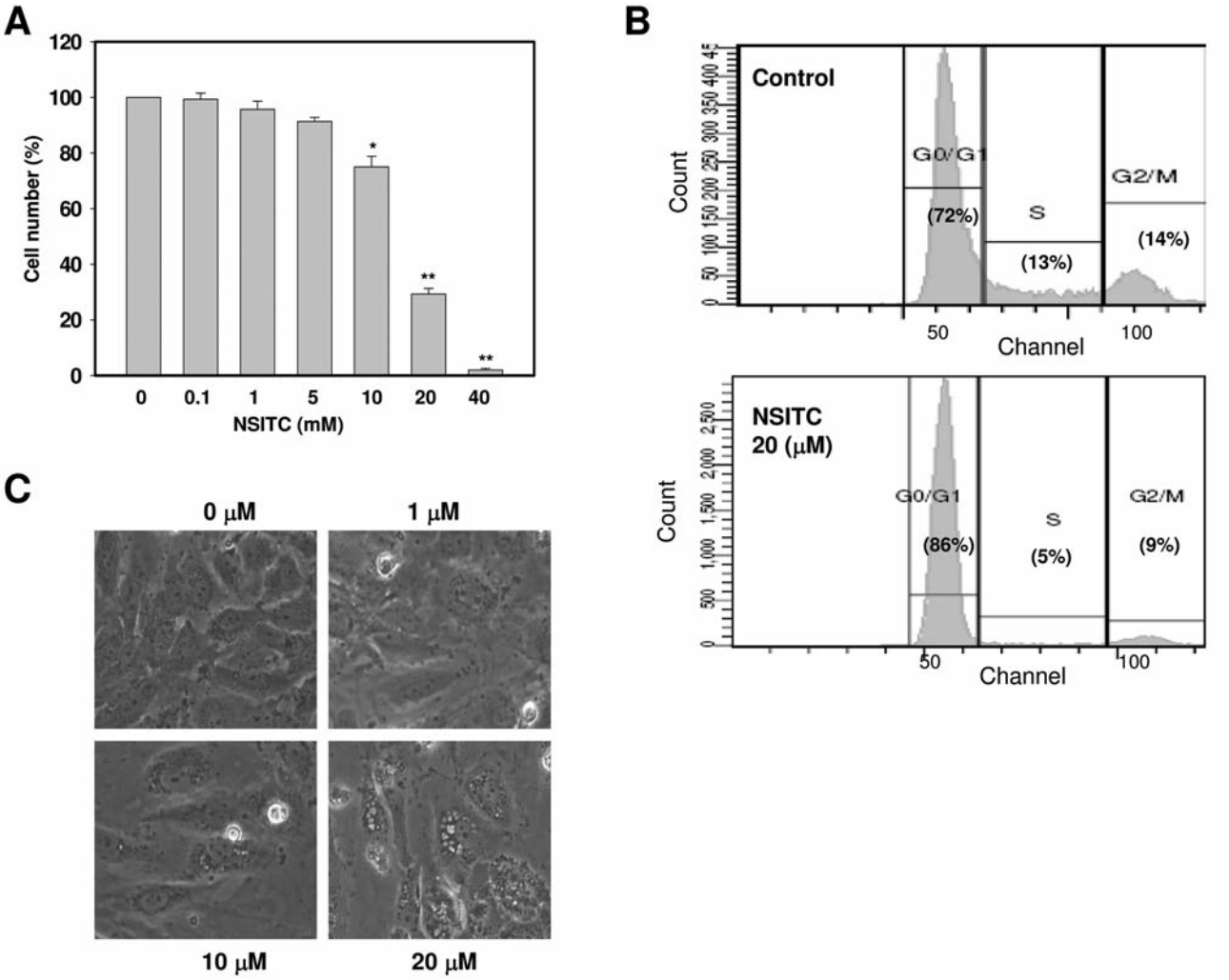

Figure 1. *Determination of endothelial cell response to NSITC. A) HUVECs were exposed to NSITC at the indicated concentrations, and after 3 days in culture, cell viability was determined by MTT assay, as described in Materials and Methods. The data represent the means±SE of three determinations. *p<0.05; **p<0.01. B) The effect of NSITC on cell cycle was determined in HUVECs after 24 hours' exposure to the compound. The cells were fixed and subjected to flow cytometry analysis. Percentage of cells in each phase of the cell cycle are indicated for each corresponding peak. C) Morphological analysis of HUVECs subjected to treatment with NSITC. The cells were exposed to the indicated concentrations for 24 hours, and then images were were obtained under light microscopy (×20 magnification).*

allowing access to the CAM. Sterile disks of no. 1 Whatman filter paper were immersed in ethanol and air dried under sterile conditions. NSITC or control solvent was applied to the disks, which were subsequently dried. The disks were then suspended in PBS and placed on the prepared CAMs. After incubation for 3 days, the CAM beneath each filter disk was harvested and rinsed with PBS. Membranes were placed in a 35-mm Petri dish and examined under an SV6 stereo microscope at ×50 magnification. Digital images were captured and analyzed with Image-Pro software (Media Cybernetics, Silver Spring, MD, USA). The number of vessel branch points within a circular region corresponding to the filter disk was counted. One image per CAM preparation was examined, and the results from 8 CAM preparations were analyzed for each treatment condition. The angiogenesis index represents the means±SEM of all results for each condition. The effect of NSITC (1.0 μg/CAM) on tumor angiogenesis and tumor growth of 1×10^6 MCF7 doxorubicin resistant (DoxR) cells implanted in matrigel in 7-day-old chick eggs was determined 8 days after implantation. Data represent the means±SEM of tumor weight (in milligrams) per treatment group and tumor hemoglobin (mg/dl), n=8 per group.

Mouse matrigel model of angiogenesis. Matrigel plug assays in mice were performed in accordance with institutional guidelines for animal safety and welfare, as previously described by our laboratory (28). Normal male mice (C57BL/6NCr) 6-8 weeks of age and weighing approximately 20 g were allowed to acclimate for 5 days prior to the initiation of treatment. Matrigel was subcutaneously injected (3 injection sites per animal) to achieve a final dose of 100 μl/animal. As

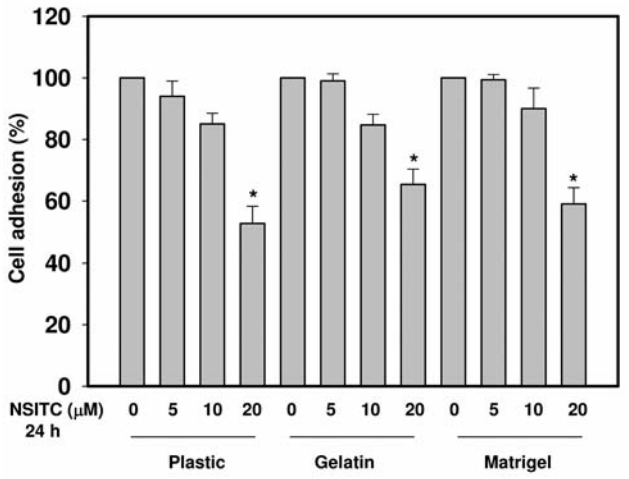

Figure 2. *Effect of NSITC on endothelial cell adhesion. HUVECs were pre-incubated for 24 hours in the absence or presence of NSITC at the indicated concentrations. Equal numbers of cells were allowed to attach to plastic gelatin or matrigel for 30 min. The attached cells were stained with 0.5% crystal violet and the percentage of adherent cells was calculated. Data represent the means±SE of three determinations. *p<0.01.*

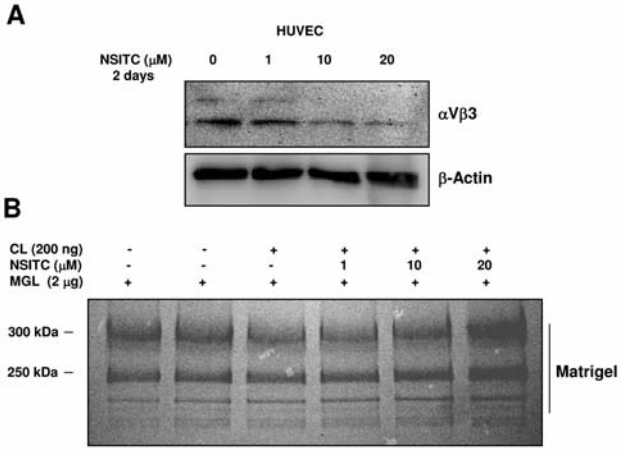

Figure 3. *Effect of NSITC on the expression of integrin αVβ3 and cathepsin L-mediated degradation of matrigel. A) HUVECs were incubated for 48 hours in the absence or presence of the indicated concentrations of NSITC. Equal amounts of protein were analyzed by Western blot using an anti-integrin αVβ3 antibody, and an antiβ-actin antibody as a control. B) Cathepsin L was incubated for 20 min at 37˚C with matrigel, in the absence or presence of increasing concentrations of NSITC. The reaction was terminated by the addition of Laemmeli buffer followed by boiling for 2 min. Proteins were separated by SDS-PAGE, and then stained with Coomassie blue. Photographs of the gel are presented.*

negative and positive controls, animals were subcutaneously injected with matrigel alone (100 μl) and with 0.1 μg FGF2 in 100 μl of matrigel, respectively. Animals in the NSITC group were subcutaneously injected with 0.1 μg of FGF2 + 10 μg of NSITC in 100 μl of matrigel. All groups consisted of 5 mice. At day 12 post plug implant, all animals were scarified and hemoglobin levels were quantified by spectrophotometry (28).

Tumor xenografts. Nude mice 6-8 weeks of age and weighing approximately 20 g (Charles River) were allowed to acclimate for 5 days prior to the start of treatment. The animals were injected with MCF7-DoxR cells (10^6 cells) subcutaneously, and after the tumors became palpable (at day 12), mice were divided into 2 groups of seven. One group received an injection of NSITC (15 mg/kg) once per day for three consecutive days, and the control group was injected similarly with vehicle alone. Tumors were measured with a caliper every day, and converted to tumor volume using the formula $W \times L^2/2$ to generate tumor growth curves.

Statistical analysis. Statistical analysis was performed by one-way ANOVA, using Statview software (Adept Scientific, Acton, MA, USA). Comparisons were made between the means±SD of branch points from each experimental group and its respective control group. Statistical significance was defined as $p<0.05$. In the CAM studies, the angiogenesis index for each treatment group was compared to that of the corresponding control group.

Results

Effect of NSITC on endothelial cell proliferation and death. The effect of NSITC on proliferation of endothelial cells was determined by subjecting HUVECs to treatment with increasing concentrations of NSITC for 72 h. As shown in Figure 1A, NSITC inhibited cellular proliferation in a dose-dependent manner, with a maximum effect at 40 μM. We previously observed that complete inhibition of cancer cell proliferation generally requires 80 μM NSITC (29). Thus, NSITC might exert anti-angiogenic effects before anticancer effects. To determine which phase of the cell cycle was affected by NSITC, HUVECs were treated with 10 μM NSITC for 24 h, then fixed and subjected to analysis by flow cytometry. As shown in Figure 1B, endothelial cell exposure to NSITC resulted in cell cycle arrest in G_0/G_1. The fraction of cells arrested in this phase increased from 72% to 86%, while the number of cells in S and G_2/M decreased respectively from 13% to 5% and from 14% to 9%. Morphologically, the cells became flattened after exposure to 1 to 10 μM NSITC, and displayed cytoplasmic vacuoles, particularly in the presence of 10 and 20 μM NSITC, which was indicative of autophagic death (29) (Figure 1C). Together, the findings suggested that NSITC is likely to have anti-angiogenic functions, as it inhibited the proliferation of endothelial cells and induced cell death by autophagy at higher concentrations.

Effect of NSITC on endothelial cell adhesion. Angiogenesis depends not only on the proliferation of endothelial cells, but

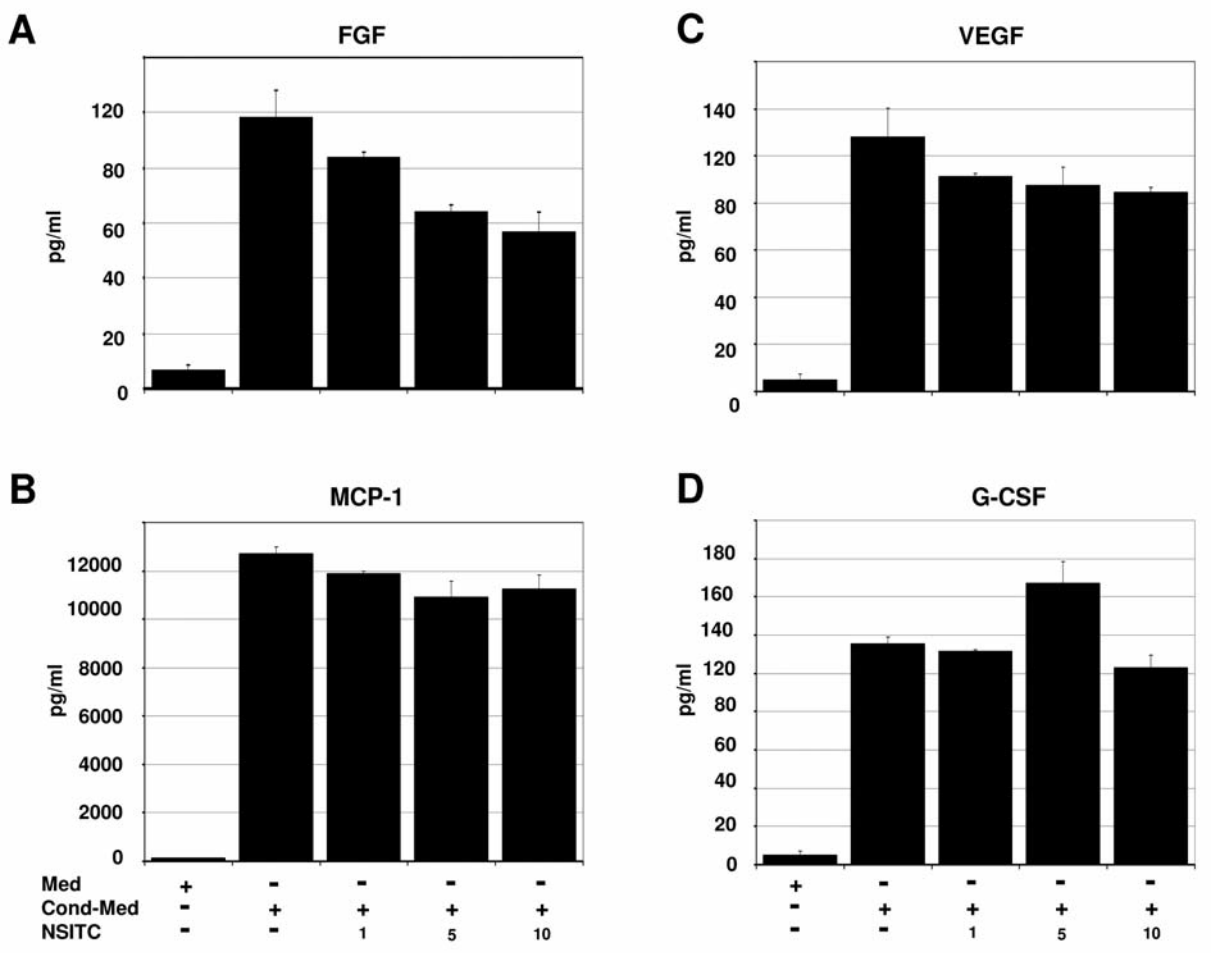

Figure 4. *Effect of NSITC on secretion of pro-angiogenic factors. HUVECs were incubated for 48 hours in the absence or presence of NSITC at the indicated concentrations (μM). The levels of FGF, VGEF, G-CSF and MCP-1 (in pg/ml) in the culture media were determined using the Bioplex assay, as described in Materials and Methods. Data represent the means±SE of four determinations.*

also on their ability to adhere to and migrate through the ECM. Here we tested the effect of NSITC on endothelial cell adhesion to different substrates, including plastic, gelatin and matrigel. The results (Figure 2) indicated that NSITC readily inhibits cell adhesion to all three substrata tested, although with different potencies. Thus, in addition to cellular proliferation, the anti-angiogenic effects of NSITC might also be mediated through the inhibition of endothelial cell adhesion to the ECM.

Putative mechanisms by which NSITC inhibits endothelial cell adhesion and motility. Cell adhesion and motility are known to be controlled by many factors, including adhesion molecules, the composition of the ECM, and the availability of pro-angiogenic factors such as VEGF and FGF. We analyzed the role of some of these factors in mediating the action of NSITC. As shown in Figure 3A, expression of the adhesion molecule αVβ3 integrin was reduced in endothelial cells treated with 10 and 20 μM NSITC. The effect of this compound on the ability of cathepsin L to degrade matrigel was also assessed *in vitro* under optimum reaction conditions for the enzyme. As shown in Figure 3B, cathepsin L was effective in degrading matrigel (band corresponding to 300 kDa), however, this activity was inhibited by the addition of NSITC. These results suggested that the anti-angiogenic effects of NSITC might be mediated in part by its ability to inhibit cathepsin L-mediated degradation of the ECM.

The effect of NSITC on endothelial cell-mediated secretion of pro-angiogenic growth factors was also analyzed. Cells were treated with increasing concentrations of inhibitor, and then allowed to incubate for 48 h. The concentrations of VEGF, FGF, G-CSF and MCP-1 were measured in culture media from treated and untreated cells using the BioPlex assay. NSITC induced a dose-dependent

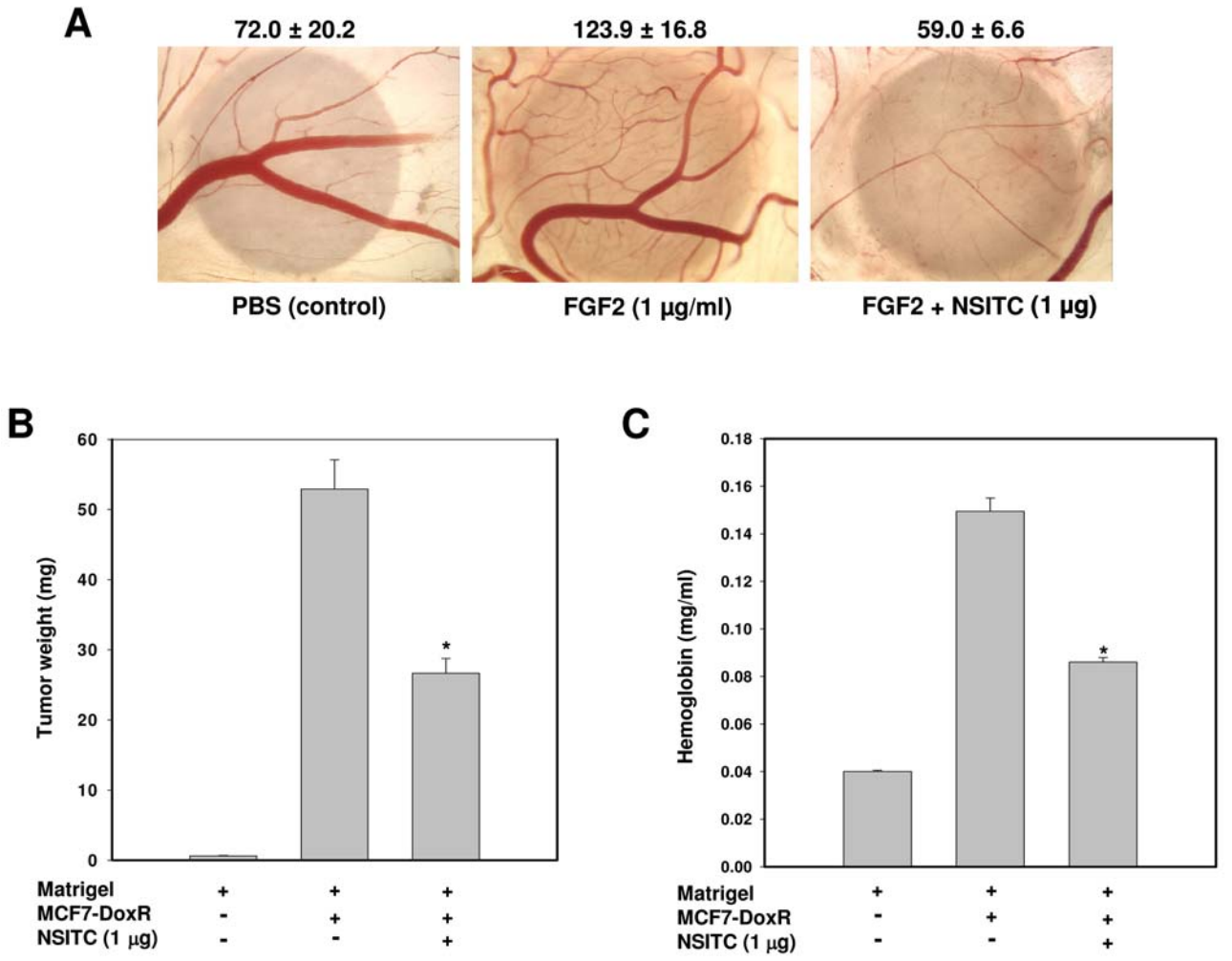

Figure 5. *Effect of NSITC on angiogenesis in FGF2- and cancer-mediated angiogenesis in the CAM model. A) An FGF-impregnated filter disk was placed over the branch point of a selected vessel in the CAM, and then NSITC was administered topically for 3 days. CAM tissue directly beneath the growth factor filter disk was removed, examined microscopically, and then images were analyzed using Image-Pro Plus software. The number of vessel branch points contained in a circular region equal to the area of the filter disk was counted for each section. The number of branch points is presented above each representative photograph. Data represent the means±SE of 8 determinations. B and C) MCF7-DoxR cells were implanted in the CAM (10^6 cells/CAM) and allowed to grow for 1 week, at which point tumor weight and hemoglobin content were determined. Data represent the means±SE of four determinations. *p<0.01.*

decrease in secreted FGF, and to a lesser extent VEGF (Figure 4). In contrast, there was no significant change in the levels of secreted G-CSF or MCP-1. Taken together, the data presented in Figures 3 and 4 suggested that NSITC may act on more than one pathway to inhibit angiogenesis.

Anti-angiogenic effects of NSITC in vivo. The effect of NSITC on microvessel formation *in vivo* was studied in the CAM model. The number of vessel branch points was determined in the absence and in the presence of inhibitor. As shown in Figure 5A, FGF2-mediated angiogenesis was completely abolished by NSITC at a concentration of 1 µg/ml, with values decreasing from 123 in the absence to 59 in the presence of compound. The proliferation of MCF7-DoxR cells in the CAM model was inhibited by NSITC (Figure 5B), and the hemoglobin content of tumors was also reduced (Figure 5C). These results provided evidence that the anti-angiogenic effects of NSITC play an important role in its anticancer activity.

Translation of these observations to the mouse model indicated that NSITC exerts a strong antitumor effect and is capable of inhibiting growth of tumors derived from MCF7-DoxR cells (Figure 6A). NSITC was also capable of inhibiting angiogenesis in the mouse model, as the

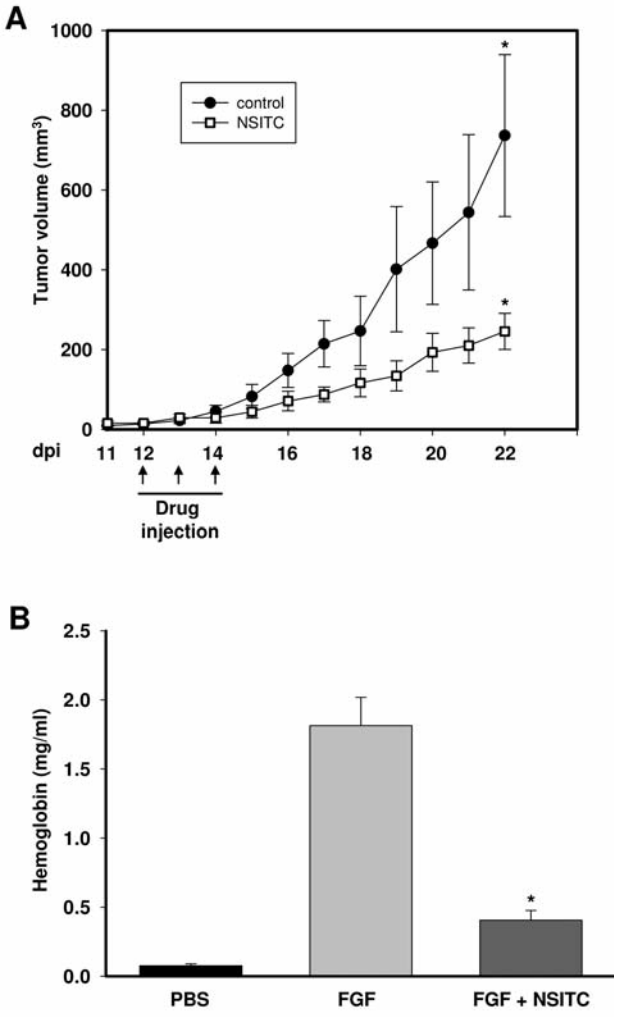

Figure 6. *Effect of NSITC on tumor growth and hemoglobin levels in mice. A) Nude mice harboring xenografts of MCF7- DoxR cells received three injections of either NSITC (15 mg/kg) or vehicle. Tumor volumes were measured starting 11 days post injection (dpi) of MCF7-DoxR cells, and continued for two weeks. The data represent the means±SE (n=7). *p<0.01. B) Mice were subcutaneously injected with Matrigel containing FGF, with or without NSITC. After 12 days, the matrigel plugs were removed and digested. Hemoglobin levels were assayed as described in Material and Methods. Data represent the means±SE (n=15). *p<0.01.*

hemoglobin levels of treated mice were much lower than those of untreated animals (Figure 6B).

Overall, the findings presented in this study provide evidence that NSITC exerts anti-angiogenic effects *in vitro* and *in vivo*, most likely by targeting both endothelial cell proliferation and interaction with the ECM. In addition to the previously described anticancer and drug-sensitizing functions of this inhibitor (19, 20, 29), these results indicate that NSITC holds great promise for the treatment of aggressive cancer.

Discussion

Cathepsins are a family of lysosomal proteases that, until recently, were considered housekeeping molecules. However, with the aid of knock-out technology, specific functions have been attributed to each one of these proteases (18). Transgenic mice lacking cathepsin L suffer from dilated cardiomyopathy (30), suggesting a critical role of this enzyme in cardiac morphogenesis and function. Neural loss and brain atrophy accompanied by early death were reported in double-knockout mice lacking both cathepsin B and L (31). Electron microscopic analysis showed that cardiomyocytes and neurons from these mice had multiple large and apparently fused lysosomes containing electron-dense non-degraded material indicative of autophagy. Cathepsin L deficiency is also associated with hair loss in mice, suggesting a role in the regulation of epithelial cell proliferation and differentiation in the skin (32). In *Caenorhabditis elegans*, cathepsin L deficiency causes embryonic lethality (15). Together, these results suggest that cathepsin L is a key determinant of cell survival.

When applied to cancer however, this function of cathepsin L would theoretically be associated with cancer progression and poor prognosis. In fact, previous work from our laboratory identified cathepsin L as a compelling target for the suppression of cancer cell resistance to chemotherapy (19, 20, 29). To date, a role for cathepsin L in cancer angiogenesis has not yet been elucidated. Here we report that NSITC, a specific cathepsin L inhibitor, acts as a potent suppressor of tumor angiogenesis *in vitro* and *in vivo*. This novel function was found to be mediated at least in part through the inhibition of proliferation and survival of endothelial cells (Figure 1A). The relatively high sensitivity of endothelial cells to NSITC (Figure 1) as compared to cancer cells (29) suggests that at low doses, this compound may act primarily to prevent angiogenesis, and consequently nutrient supply to tumors. In the current study, at low concentrations, NSITC suppressed endothelial cell proliferation through cell cycle arrest at the G_0/G_1 phase (Figure 1B). In contrast, high concentrations (20 to 40 μM) of NSITC induced cell death reminiscent of autophagy (Figure 1C). Thus, while NSITC may be effective in suppressing tumor progression at low concentrations, at higher doses, it may cause tumors to shrink.

NSITC effectively reduced cell attachment to plastic, gelatin and matrigel (Figure 2), indicating that it can disrupt endothelial cell adhesion. Thus, the possibility exists that the anti-angiogenic effects of NSITC are mediated either by direct action on endothelial cells (for example, by inhibiting the expression of adhesion molecules), or indirectly, by preventing cathepsin L-mediated degradation of the ECM. Our results do not rule out either of these mechanisms, in that the expression of αVβ3 integrin was reduced in endothelial

cells treated with NSITC (Figure 3A), and cathepsin L-mediated degradation of matrigel was reduced in the presence of inhibitor (Figure 3B). NSITC also inhibited the secretion of the pro-angiogenic factors FGF and VEGF (Figure 4A and 4C), providing support for a direct mechanism of action of NSITC on endothelial cells. While the molecular details of the mechanism of action of NSITC remain to be fully elucidated, our findings indicate that NSITC acts on more than one pathway implicated in angiogenesis, and mostly likely because of this, dramatically suppressed angiogenesis in the CAM and mouse models (Figures 5 and 6). Along with our previous findings that NSITC acts directly on cancer cells to enhance their sensitivity to chemotherapeutic agents (19, 20), the current results implicate NSTIC as a compelling drug candidate for the treatment of aggressive cancer.

Acknowledgements

This work was supported in part by the National Cancer Institute (1R41 CA128152-01 to S.A.M.). The authors wish to thank Drs. Patricia Phillips and Mary Rose Burnham for help in the preparation of this manuscript.

References

1 Folkman J: Role of angiogenesis in tumor growth and metastasis. Semin Oncol *29*: 15-18, 2002.

2 Folkman J: Angiogenesis inhibitors: a new class of drugs. Cancer Biology & Therapy *2*: S127-133, 2003.

3 Verhoef C, de Wilt JH and Verheul HM: Angiogenesis inhibitors: perspectives for medical, surgical and radiation oncology. Current Pharmaceutical Design *12*: 2623-2630, 2006.

4 Folkman J:Angiogenesis. Ann Rev Med *57*: 1-18, 2006.

5 Pepper MS: Extracellular proteolysis and angiogenesis. Thrombosis and Haemostasis *86*: 346-355, 2001.

6 Deryugina EI and Quigley JP: Matrix metalloproteinases and tumor metastasis. Cancer Metastasis Reviews *25*: 9-34, 2006.

7 Stetler-Stevenson WG: Matrix metalloproteinases in angiogenesis: a moving target for therapeutic intervention. J Clin Invest *103*: 1237-1241, 1999.

8 Wagenaar-Miller RA, Gorden L and Matrisian LM: Matrix metalloproteinases in colorectal cancer: is it worth talking about? Cancer Metastasis Reviews *23*: 119-135, 2004.

9 Heath EI, Burtness BA, Kleinberg L, Salem RR, Yang SC, Heitmiller RF, Canto MI, Knisely JP, Topazian M, Montgomery E, Tsottles N, Pithavala Y, Rohmiller B, Collier M and Forastiere AA: Phase II, parallel-design study of preoperative combined modality therapy and the matrix metalloprotease (mmp) inhibitor prinomastat in patients with esophageal adenocarcinoma. Investigational New Drugs *24*: 135-140, 2006.

10 Fingleton B: MMPs as therapeutic targets – still a viable option? Seminars in Cell & Developmental Biology 19:61-8, 2008.

11 Duffy MJ: Proteases as prognostic markers in cancer. Clin Cancer Res *2*: 613-618, 1996.

12 Lah TT and Kos J: Cysteine proteinases in cancer progression and their clinical relevance for prognosis Biol Chem *379*: 125-130, 1998.

13 Joyce JA, Baruch A, Chehade K, Meyer-Morse N, Giraudo E, Tsai FY, Greenbaum DC, Hager JH, Bogyo M and Hanahan D: Cathepsin cysteine proteases are effectors of invasive growth and angiogenesis during multistage tumorigenesis. Cancer Cell *5*: 443-453, 2004.

14 Gocheva V and Joyce JA: Cysteine cathepsins and the cutting edge of cancer invasion. Cell Cycle *6*: 60-64, 2007.

15 Hashmi S, Britton C, Liu J, Guiliano DB, Oksov Y and Lustigman S: Cathepsin L is essential for embryogenesis and development of *Caenorhabditis elegans*. J Biol Chem *277*: 3477-3486, 2002.

16 Kane SE and Gottesman MM: The role of cathepsin L in malignant transformation. Semin Cancer Biol *1*: 127-136, 1990.

17 Rousselet N, Mills L, Jean D, Tellez C, Bar-Eli M and Frade R: Inhibition of tumorigenicity and metastasis of human melanoma cells by anti-cathepsin L single chain variable fragment. Cancer Res *64*: 146-151, 2004.

18 Gocheva V, Zeng W, Ke D, Klimstra D, Reinheckel T, Peters C, Hanahan D and Joyce JA: Distinct roles for cysteine cathepsin genes in multistage tumorigenesis. Genes Dev *20*: 543-556, 2006.

19 Zheng X, Chou PM, Mirkin BL and Rebbaa A: Senescence-initiated reversal of drug resistance: specific role of cathepsin L. Cancer Res *64*: 1773-1780, 2004.

20 Zheng X, Chu F, Chou PM, Gallati C, Dier U, Mirkin BL, Mousa SA and Rebbaa A: Cathepsin L inhibition suppresses drug resistance *in vitro* and *in vivo*: a putative mechanism. Am J Physiol *296*: C65-74, 2009.

21 Lombardi G, Burzyn D, Mundinano J, Berguer P, Bekinschtein P, Costa H, Castillo LF, Goldman A, Meiss R, Piazzon I and Nepomnaschy I: Cathepsin-L influences the expression of extracellular matrix in lymphoid organs and plays a role in the regulation of thymic output and of peripheral T-cell number. J Immunol *174*: 7022-7032, 2005.

22 Yasuma T, Oi S, Choh N, Nomura T, Furuyama N, Nishimura A, Fujisawa Y and Sohda T: Synthesis of peptide aldehyde derivatives as selective inhibitors of human cathepsin L and their inhibitory effect on bone resorption. J Med Chem *41*: 4301-4308, 1998.

23 Rebbaa A, Chou PM and Mirkin BL: Factors secreted by human neuroblastoma mediated doxorubicin resistance by activating STAT3 and inhibiting apoptosis. Mol Med *7*: 393-400, 2001.

24 Chuan YC, Pang ST, Cedazo-Minguez A, Norstedt G, Pousette A and Flores-Morales A: Androgen induction of prostate cancer cell invasion is mediated by ezrin. J Biol Chem *281*: 29938-29948, 2006.

25 Davis FB, Mousa SA, O'Connor L, Mohamed S, Lin HY, Cao HJ and Davis PJ: Proangiogenic action of thyroid hormone is fibroblast growth factor-dependent and is initiated at the cell surface. Circ Res *94*: 1500-1506, 2004.

26 Davis FB, Tang HY, Shih A, Keating T, Lansing L, Hercbergs A, Fenstermaker RA, Mousa A, Mousa SA, Davis PJ and Lin HY: Acting *via* a cell surface receptor, thyroid hormone is a growth factor for glioma cells. Cancer Res *66*: 7270-7275, 2006.

27 Mousa SA, O'Connor LJ, Bergh JJ, Davis FB, Scanlan TS and Davis PJ: The proangiogenic action of thyroid hormone analogue GC-1 is initiated at an integrin. J Cardiovasc Pharmacol *46*: 356-360, 2005.

28 Powell JA, Mohamed SN, Kerr JS, Mousa SA: Antiangiogenesis efficacy of nitric oxide donors. J Cell Biochem *80*: 104-114, 2000.

29 Zheng X, Chu F, Mirkin BL, Sudha T, Mousa SA and Rebbaa A: Role of the proteolytic hierarchy between cathepsin L, cathepsin D and caspase-3 in regulation of cellular susceptibility to apoptosis and autophagy. Biochim Biophys Acta *1783*: 2294-2300, 2008.

30 Stypmann J, Glaser K, Roth W, Tobin DJ, Petermann I, Matthias R, Mönnig G, Haverkamp W, Breithardt G, Schmahl W, Peters C and Reinheckel T: Dilated cardiomyopathy in mice deficient for the lysosomal cysteine peptidase cathepsin L. Proc Natl Acad Sci USA *99*: 6234-6239, 2002.

31 Felbor U, Kessler B, Mothes W, Goebel HH, Ploegh HL, Bronson RT and Olsen BR: Neuronal loss and brain atrophy in mice lacking cathepsins B and L. Proc Natl Acad Sci USA *99*: 7883-7888, 2002.

32 Benavides F, Starost MF, Flores M, Gimenez-Conti IB, Guenet JL and Conti CJ: Impaired hair follicle morphogenesis and cycling with abnormal epidermal differentiation in nackt mice, a cathepsin L-deficient mutation. Am J Pathol *161*: 693-703, 2002.

Received June 2, 2009
Revised September 9, 2009
Accepted September 28, 2009